Electronic Supplementary Material (ESI) for ChemComm.

Supporting Information

Isolation and Characterization of [5,6]-Pyrrolidino-$Sc_3N@C_{80}$ Diastereomers

Yutaka Maeda,* Masato Kimura, Chihiro Ueda, Michio Yamada, Toru Kikuchi, Mitsuaki Suzuki, Wei-Wei Wang, Naomi Mizorogi, Nikolaos Karousis, Nikos Tagmatarchis, Tadashi Hasegawa, Marilyn M. Olmstead, Alan L. Balch, Shigeru Nagase, Takeshi Akasaka*

Experimental section

Fig. S1 HPLC profiles of reaction mixture of $Sc_3N@I_h$-C_{80} with **1a** (red). Conditions: 4.6 mm × 250 mm i.d. 5PYE columns; eluent, toluene 1.0 mL/min.

Fig. S2 HPLC profiles of **2a** and **3a**. Conditions: 5NPE column, toluene 1.0 $mLmin^{-1}$, 330 nm detection

Fig. S3 Mass spectra of **2a** and **3a** in negative mode using TPB as a matrix.

Fig. S4 Absorption spectra of **2** and **3** in CS2.

Fig. S5 ^1H NMR spectra of **2a** and **3a** in $CDCl_3$:CS_2 = 1:1 (v/v), 125 MHz, 293 K.

Fig. S6 ^{13}C NMR spectra of **2a** and **3a** in $CDCl_3$:CS_2 = 1:1 (v/v), 125 MHz, 293 K.

Fig. S7 DEPT-135 NMR spectra of **2a** and **3a** in $CDCl_3$:CS_2 = 1:1 (v/v), 125 MHz, 293 K.

Fig. S8 HMBC spectrum of **2a** and **3a** in $CDCl_3$:CS_2 = 1:1 (v/v), 125 MHz, 293 K.

Fig. S9 Drawings of (a) the independent unit (**2a**) in the unit cell that exists on the crystallographic mirror and (b & c) two disorder orientations of the independent unit. Their orientations have the relation of chiral and 0.50 occupancies, respectively.

Fig. S10 HPLC profiles of reaction mixture of $Sc_3N@I_h$-C_{80} with **1b** (red). Conditions: 4.6 mm × 250 mm i.d. Buckyprep-M columns; eluent, toluene 1.0 mL/min.

Fig. S11 HPLC profiles of **2b** and **3b**. Conditions: 5NPE column, toluene 1.0 $mLmin^{-1}$, 330 nm detection.

Fig. S12 Mass spectra of **2b** and **3b** in negative mode using TPB as a matrix.

Fig. S13 ^1H NMR spectra of **2b** and **3b** in $CDCl_3$:CS_2 = 1:1 (v/v), 400 MHz, 298 K.

Fig. S14 ^{13}C NMR spectra of **2b** and **3b** in $CDCl_3$:CS_2 = 1:1 (v/v), 125 MHz, 298 K.

Fig. S15 DEPT-135 ^{13}C NMR spectra (125 MHz) of **2b** and 3**b** measured in CS_2/$CDCl_3$ (1:1) at 298K.

Fig. S16 HSQC NMR spectrum of **2b** measured in CS_2/$CDCl_3$ (1:1) at 298K.

Fig. S17 HMBC NMR spectrum of **2b** measured in CS_2/$CDCl_3$ (1:1) at 298K.

Fig. S18 HSQC NMR spectrum of **3b** measured in CS_2/$CDCl_3$ (1:1) at 298K.

Fig. S19 HMBC NMR spectrum of **3b** measured in CS_2/$CDCl_3$ (1:1) at 298K.

Fig. S20 CV and DPV curves of **2a**, **2b**, **3a**, and **3b** in ODCB.

Fig. S21 Optimized structures for [5,6]- and [6,6]-pyrrolidino-$Sc_3N@I_h$-C_{80} calculated at M06-2X/6-31G(d)[C,H,N,O], LanL2DZ[Sc] level.

Fig. S22 Optimized structures for [5,6]-pyrrolidino-$Sc_3N@I_h$-C_{80} calculated at M06-2X/6-31G(d)[C,H,N,O], LanL2DZ[Sc] level.

Fig. S23 HPLC profiles of (pyrrolidino)$_n$-$Sc_3N@I_h$-C_{80} in the presence of maleic unhydride at 180˚C for 24 h. Column: Buckyprep 4.6 ϕ × 250 mm, 40°C, eluent: toluene 1.0mL/min.

Fig. S24 Negative-mode MALDI-TOF mass spectra of (a) (pyrrolidino)$_n$-$Sc_3N@I_h$-C_{80} and (b) (pyrrolidino)$_n$-$Sc_3N@I_h$-C_{80} treated at 180˚C for 24 h in the presence of maleic unhydride. matrix: 1,1,4,4-tetraphenyl-1,3-butadiene.

Experimental Section

***General*:**

$Sc_3N@I_h$-C_{80} was purchased from Luna Innovations. Chemicals and solvents were reagent grade and purchased from Aldrich Chemical Co. Inc, Wako Pure Chemical Industries Ltd., and Tokyo Chemical Industry Co., Ltd. $Sc_3N@I_h$-C_{80} was isolated from an isomeric mixture of $Sc_3N@I_h$-C_{80} and $Sc_3N@D_{5h}$-C_{80} by preparative high-performance column chromatography (HPLC). 1,2-dichlorobenzene (ODCB) was distilled over P_2O_5 under vacuum. CS_2 was distilled over P_2O_5 under an argon atmosphere. HPLC was performed using chromatographs (LC-9201 and LC-918; Japan Analytical Industry Co. Ltd.) that were monitored using UV absorption at 330 nm. NMR measurements were conducted on spectrometers (JEOL EC-400P; JEOL Resonance Inc. and Bruker AVANCE-300 and 500; Bruker Analytik GmbH, with a CryoProbe system; Bruker Biospin K.K.). Mass spectroscopy was performed (Bruker Autoflex III and Bruker BIFLEX III; Bruker Daltonics Inc.) with 1,1,4,4-tetraphenyl-1,3-butadiene (TPB) as the matrix. The Vis/NIR absorption spectra were measured using spectrophotometers (V-670 spectrophotometer; JASCO Inc. and UV-3150; Shimadzu Corp.). Cyclic voltammograms (CVs) and differential pulse voltammograms (DPVs) were recorded on electrochemical analyzers (HZ-5000 Automatic Polarization System; Hokuto Denko Corp. and CV50W; BAS Inc.) filled with 0.1 M $(n\text{Bu})_4\text{NPF}_6$ in ODCB. Platinum wires were used as the working electrode and the counter electrode. The reference electrode was a saturated calomel reference electrode (SCE). All potentials were referenced to the ferrocene/ferrocenium couple (Fc/Fc^+) as the standard. CV: scan rate, 20 mVs^{-1}. DPV: pulse amplitude, 50 mV; pulse width, 50 ms; pulse period, 200 ms; scan rate, 20mVs^{-1}.

Theoretical calculations:

Theoretical calculations were carried out by using the Gaussian 09 program suite revision A and C[1] with density functional theory at the M06-2X level.[2]The 6-31G(d) basis[3] set on C, H, N, O atoms and the LANL2DZ basis set[4] on Sc atoms were used. The ^{1}H NMR chemical shifts were calculated by using the M06-2X-GIAO method[5] using 6-31G(d) basis set on C, H, N, O atoms and the LANL2DZ basis set on Sc atoms.

Single-crystal X-ray structure analysis:

Black crystals of **2a** were obtained by diffusion of hexane into carbon disulfide solution of **2a** in glass tube (ϕ = 8 mm) at 273 K for about one month. X-ray data were collected at 90 K by using a SMART APEX II ULTRA (Bruker AXS, Germany) equipped with a detector (APEX II CCD; Bruker AXS, Germany). The structure was solved by direct methods and refined by using SHELXL-2014.[6]

The structure was refined as a two-component twin. The I_h-C_{80} cage, together with its substituent group, is disordered into two orientations. These atoms were refined anisotropically at 0.50/0.50 occupancy. Restraints of SIMU, EADP, ISOR, EXYZ, SADI and DFIX commands were applied due to large thermal motion, certain overlapping atoms of the disordered parts, and related geometric distortions. Six Sc atom site were assigned. They are divided into two parts. One part includes Sc1, Sc2, and Sc3. The other part includes Sc4, Sc5, and Sc6. The two parts were refined anisotropically with 0.50 occupancy each. This structure has disordered solvent (CS2/hexane) which could not be adequately modeled. Therefore, the refinement used SQUEEZE/PLATON. The solvent regions accounted for approximately 65 unassigned electrons. Additional details can be found in the electronic supporting information as a CIF.

It is not possible to associate one of the two sets of three Sc's with a particular cage orientation based only on the occupancies because the two different cage orientations and the two different Sc_3N orientations are both in ratios of 0.50/0.50. However, previous work on [5,6]-adducts of $Sc_3N@I_h$-C_{80} indicates that there is a preferential position for the Sc's that avoids the site of addition and aligns the top line of the "Y" with the line of the carbon atoms at the site of addition.[7] Therefore, we have associated Sc1, Sc2 and Sc3 with the first residue of C_{80} and Sc4, Sc5 and Sc6 with the second residue of C_{80}. The first pairing is depicted in Figure 3. The distances Sc2$\cdots$C1 and Sc3$\cdots$C2 are 3.459(2) and 3.496(2) Å, respectively. The C1-C2 distance of 1.600(19) Å clearly indicates that the cage remains

"closed." Similar values are observed for the other pairing. It is notable that the disorder in the orientations of the two cages differs from similar [5,6] adducts where the 5- and 6-membered rings simply exchange positions at the site of addition. In the present case, the rotation of the C1-C2 bond is ca. 70° rather than 180°.

Synthetic Procedures:
Methyl 1-*tert*-butylaziridine-2-carboxylate (**1a**) and methyl ethyl 1-*n*-octylaziridine-2-carboxylate (**1b**) were synthesized according to literature procedures.[8]

Methyl 1-*tert*-butylaziridine-2-carboxylate (**1a**). To a solution of methyl 2,3-dibromopropionate (3.6 mL, 28.5 mmol) in tetrahydrofuran (70 mL) cooled at 0˚C was added dropwise a tetrahydrofuran solution (70 mL) of *tert*-butylamine (2.98 mL, 28.4 mmol) and triethylamine (7.96 mL, 57.8 mmol). After stirring at room temperature for 17 h the white precipitate formed was filtered off to yield an orange solution and the filtrate was purified by column chromatography with ethyl acetate/*n*-hexane (v/v = 5:1) and ethanol as eluents to afford the compound **1a**. (0.23 g, 5%).

Ethyl 1-*n*-octylaziridine-2-carboxylate (**1b**).
To a solution of methyl 2,3-dibromopropionate (1.4 mL, 9.62 mmol) in tetrahydrofuran (37.5 mL) cooled at 0˚C was added dropwise a tetrahydrofuran solution (37.5 mL) of *n*-octylamine (1.5 mL, 9.62 mmol) and triethylamine (2.7 mL, 19.2 mmol). After stirring at room temperature for 12 h the white precipitate formed was filtered off and the crude product was purified by column chromatography with ethyl acetate/*n*-hexane (v/v = 1:1) to afford the compound **1b**. (1.9 g, 87%).

Preparation of [5,6]-pyrrolodino-$Sc_3N@I_h$-C_{80} (**2a**)
An ODCB solution (5 ml) of $Sc_3N@I_h$-C_{80} (1.0 mg, 9×10^{-4} mmol) and **1a** (15.4 mg, 9×10^{-2} mmol) was placed in a Pyrex tube and degassed through freeze–pump–thaw cycles under reduced pressure. The mixture was stirred at 180˚C for 1 h. After removal of solvent under vacuum, the residue was dissolved in toluene and injected into an HPLC for analysis. Mono-adducts (**2a** and **3a**) and $Sc_3N@I_h$-C_{80} were isolated using HPCL with a Buckyprep column (20 mm x 250 mm i.d.; Cosmosil; Nacalai Tesque Inc.) eluted with toluene at 9.9 mL min^{-1}. The conversion yield of **2a** (26%) and **3a** (18%) was calculated from the HPLC peak area assuming that $Sc_3N@I_h$-C_{80} and the monoadducts have the same ε values.

Data for 2a: Dark brown solid. ^{1}H NMR (500 MHz, CS_2/$CDCl_3$ (1:1), 293 K) δ 4.81(s,1H,-C<u>H</u>-), 4.19(d, J = 8.8 Hz, 1H, -CH<u>H</u>-), 4.02(d, J = 8.8 Hz, 1H,-C<u>H</u>H-), 3.56(s, 3H, -OC<u>H$_3$</u>), 1.43(s, 9H,-C(C<u>H$_3$</u>)$_3$ ppm; ^{13}C NMR (125 MHz, $CDCl_3$/CS_2 (1:1), 293 K) δ 173.0, 158.8, 158.6, 157.7, 156.1, 155.0, 154.8, 153.5, 150.4, 150.3, 149.6, 149.6, 149.2, 149.0, 148.5, 148.2, 147.6, 147.5, 145.5, 145.4, 144.9, 144.8, 144.2, 144.1, 144.1, 144.0, 143.7, 143.5, 143.0, 143.0, 142.2, 142.0, 141.7, 140.8, 140.8, 140.6, 140.4, 140.4, 140.4, 140.3, 140.3, 140.1, 140.0, 139.3, 139.2, 139.1, 139.1, 138.9, 138.9, 138.6, 138.5, 138.3, 138.3, 138.2, 137.8, 137.1, 137.1, 136.6, 136.2, 136.2, 136.1, 135.0, 135.0, 133.5, 133.4, 133.3, 133.1, 131.6, 131.0, 130.7, 130.5, 130.5, 130.4, 129.0, 129.0, 116.2, 116.1, 113.8, 111.0, 72.8, 62.2, 59.8, 57.6, 53.0, 51.9, 28.9 ppm; MALDI-TOF mass (negative mode, matrix = TPB): *m/z* 1266.82 ([M^-], calcd. for $C_{88}H_{15}O_2N_2Sc_3^-$:1266.99).

Crystal Data for 2a: $C_{88}H_{15}N_2O_2Sc_3$; Mr = 1266.90; 0.280 x 0.160 x 0.120 mm; monoclinic; space group $P2_1/c$ (#14); a = 11.156(4) Å; b = 21.026(6) Å; c = 21.582(7) Å; β = 96.297(4)˚; V = 5032(3) Å^3; Z = 4; T = 90 K; $\rho_{calcd.}$ = 1.672 g cm^{-3}; λ = 0.71073 Å; $\mu(Mo_{K\alpha})$ = 0.462 mm^{-1}; θ = 4.15-28.23˚; R_1 = 0.1587, wR2 = 0.3595 for all data; R_1 = 0.1246, wR_2 = 0.3595 for 27590 reflections ($I > 2.0\sigma(I)$) with 1549 parameters refined by using 1803 restraints. Crystallographic data have been deposited in the Cambridge Crystallographic Data Center (CCDC 1010741).

Data for 3a: Dark brown solid. ^{1}H NMR (500 MHz, CS_2/$CDCl_3$ (1:1), 293 K) δ 4.40(d, J = 9.5 Hz, 1H, -C<u>H</u>H-), 4.24(s, 1H, -C<u>H</u>-), 4.02(s, 3H, -OC<u>H</u>$_3$), 3.56(d, J = 9.5 Hz, 1H, -CH<u>H</u>-), 1.31(s, 9H, -C(C<u>H</u>$_3$)$_3$) ppm; ^{13}C NMR (125 MHz, $CDCl_3$/CS_2 (1:1), 293 K) δ 172.2, 158.8, 158.7, 156.3, 155.0, 154.9, 152.8, 150.4, 150.4, 149.6, 149.4, 149.3, 148.9, 148.4, 148.2, 147.7, 147.5, 145.5, 145.3, 144.8, 144.8, 144.1, 144.1, 143.9, 143.8, 143.4, 143.1, 142.7, 142.2, 141.8, 141.6, 140.9, 140.8, 140.5, 140.5, 140.4, 140.2, 140.1, 139.8, 139.4, 139.2, 139.2, 139.0, 138.9, 138.6, 138.3, 138.1, 137.8, 137.8, 137.7, 137.4, 137.2, 137.1, 136.6, 136.5, 136.3, 136.1, 135.0, 134.9, 133.6, 133.5, 133.3, 133.2, 132.0, 131.8, 130.7, 130.7, 130.6, 130.3, 129.0, 128.9, 128.9, 128.5, 128.2, 125.2, 116.0, 115.9, 113.0, 112.2, 74.6, 62.6, 61.8, 56.4, 53.6, 52.3, 27.4 ppm; MALDI-TOF mass (negative mode, matrix = TPB): *m/z* 1266.88 ([M^-], calcd. for $C_{88}H_{15}O_2N_2Sc_3^-$:1266.99).

Data for 2b: Dark brown solid. ^{1}H NMR (400 MHz, CS_2/$CDCl_3$ (1:1), 293 K): δ 4.58 (s, 1H; NCHCO), 4.1–4.2 (m, 2H; OCH_2), 4.05 (d, J = 9.2Hz, 1H; -C<u>H</u>H), 3.90 (d, J = 9.2Hz, 1H; -CH<u>H</u>), 3.0-3.1 (m, 1H; -NC<u>H</u>H(CH_2)$_6$-), 2.9-2.9 (m, 1H; -NCH<u>H</u>(CH_2)$_6$-), 1.8–1.9 (m, 2H; -NCH_2C<u>H</u>$_2$), 1.3–1.6 (m, 10H; -(C<u>H</u>$_2$)$_5$-CH_3), 1.12 (t, J = 7.1 Hz, 3H; -OCH_2C<u>H</u>$_3$), 0.97 (t, J = 6.9 Hz, 3H; -C<u>H</u>$_3$) ppm; ^{13}C NMR (125 MHz, CS_2/$CDCl_3$ (1:1), 293 K): δ 168.2, 158.0, 157.9, 157.0, 155.3, 154.2, 154.0, 152.1, 149.6, 149.6, 148.8, 148.8, 148.4, 148.3, 147.6, 147.4, 146.9, 146.7, 144.7, 144.5, 144.0, 144.0, 143.4 (2C), 143.3, 143.2, 143.0, 142.7, 142.2, 142.2, 141.4, 141.2, 141.0, 140.0, 139.9, 139.8, 139.7, 139.6, .139.6, 139.5, 139.2, 138.7, 138.5, 138.4, 138.4, 138.3, 138.2, 138.1, 137.7, 137.6, 137.5, 137.4, 137.3, 137.1, 136.4, 136.3, 135.8, 135.4, 135.4, 135.3, 134.3, 134.2 (2C), 132.7 (2C), 132.6, 132.4, 130.9, 130.6, 130.0, 129.9, 129.8, 129.8, 128.3, 128.3, 115.1, 115.0, 112.7, 110.6, 76.0, 65.2, 60.6, 59.9, 56.5, 49.3, 31.3, 29.1, 28.9, 28.7, 28.0, 26.8, 25.0, 22.2, 22.1, 13.4, 13.3 ppm; MALDI-TOF mass (negative mode, matrix = TPB): *m/z* 1336.28 ([M^-], calcd. for $C_{93}H_{25}O_2N_2Sc_3^-$:1336.06).

Data for 3b: ^{1}H NMR (400 MHz, CS_2/$CDCl_3$ (1:1), 293 K): δ 4.5–4.6 (m, 2H; OC<u>H</u>H), 4.4–4.5 (m, 2H; OCH<u>H</u>), 4.39 (d, J = 9.6 Hz, 1H; -C<u>H</u>H), 3.67 (s, 1H; NC<u>H</u>CO), 3.1-3.2 (m, 1H; -NC<u>H</u>H-(CH_2)$_6$-), 2.90 (d, J = 9.6 Hz, 1H; -CH<u>H</u>-), 2.4–2.5 (m, 1H; -NCH<u>H</u>-(CH_2)$_6$-), 1.7–1.9 (m, 2H; -NCH_2C<u>H</u>$_2$), 1.4–1.6 (m, 10H; -(C<u>H</u>$_2$)$_5$-CH_3), 0.90–0.98 (m, J = 7.3Hz, 6H; -C<u>H</u>$_3$ and -OCH_2C<u>H</u>$_3$) ppm; ^{13}C NMR (125 MHz, CS_2/$CDCl_3$ (1:1), 293 K): δ 167.8 (-<u>C</u>OO), 157.6, 157.4, 155.1, 153.9, 153.8, 152.8, 149.3, 149.3, 148.6, 148.5, 148.2, 147.9, 147.3, 147.2, 146.6, 146.4, 144.4, 144.3, 143.8, 143.7, 143.2, 143.1, 143.0, 142.9, 142.7, 142.5, 142.0, 141.8, 141.2, 140.9, 140.9, 140.5, 139.7, 139.7, 139.6, 139.4, .139.3, 139.2, 138.8, 138.2, 138.2 (2C), 138.0, 138.0, 137.7, 137.6, 137.4, 137.3, 136.8 (2C), 136.8, 136.2, 136.1, 135.6, 135.4 (2C), 134.8, 134.0, 134.0, 133.7, 132.5 (2C), 132.1, 132.0, 131.1, 130.6, 129.7, 129.6 (2C), 129.6, 129.4, 129.4, 128.1, 128.0, 127.6, 114.5, 114.3, 112.8, 111.4, 80.3, 66.9, 60.8, 60.1, 55.8, 52.2, 31.0, 28.6, 28.4, 27.1, 26.7, 21.9, 13.4, 13.1 ppm; MALDI-TOF mass (negative mode, matrix = TPB): *m/z* 1336.17 ([M^-], calcd. for $C_{93}H_{25}O_2N_2Sc_3^-$:1336.06).

References

[1] M. J. Frisch, G. W. Trucks, H. B. Schlegel, G. E. Scuseria, M. A. Robb, J. R. Cheeseman, G. Scalmani, V. Barone, B. Mennucci, G. A. Petersson, H. Nakatsuji, M. Caricato, X. Li, H. P. Hratchian, A. F. Izmaylov, J. Bloino, G. Zheng, J. L. Sonnenberg, M. Hada, M. Ehara, K. Toyota, R. Fukuda, J. Hasegawa, M. Ishida, T. Nakajima, Y. Honda, O. Kitao, H. Nakai, T. Vreven, Jr. J. A. Montgomery, J. E. Peralta, F. Ogliaro, M. Bearpark, J. J. Heyd, E. Brothers, K. N. Kudin, V. N. Staroverov, R. Kobayashi, J. Normand, K. Raghavachari, A. Rendell, J. C. Burant, S. S. Iyengar, J. Tomasi, M. Cossi, N. Rega, J. M. Millam, M. Klene, J. E. Knox, J. B. Cross, V. Bakken, C. Adamo, J. Jaramillo, R. Gomperts, R. E. Stratmann, O. Yazyev, A. J. Austin, R. Cammi, C. Pomelli, J. W. Ochterski, R. L. Martin, K. Morokuma, V. G. Zakrzewski, G. A. Voth, P. Salvador, J. J. Dannenberg, S. Dapprich, A. D. Daniels, O. Farkas, J. B. Foresman, J. V. Ortiz, J. Cioslowski and D. J. Fox, Gaussian 09, Revision C.01, Gaussian, Inc., Wallingford CT, 2009.

[2] Y. Zhao and D. G. Truhlar, *J. Phys. Chem. A,* 2005, **109**, 5656-5667.

[3] Y. Zhao and D. G. Truhlar, *Theor. Chem. Acc.,* 2008, **120**, 215-241.

[4] P. J. Hay and W. R. Wadt, *J. Phys. Chem.,* 1972, **56**, 2257-2261.

[5] K. Wolinski, J. F. Hilton and P. Pulay, *J. Am. Chem. Soc.,* 1990, **112**, 8251-8260.

[6] G. Sheldrick, *Acta Crystallogr. Sect. A*, 2008, **64**, 112-122.

[7] F.-F. Li, J. R. Pinzón, B. Q. Mercado, M. M. Olmstead, A. L. Balch and L. Echegoyen, *J. Am. Chem. Soc.,* 2011, **133**, 1563-1571.

[8] F. G. Brunetti, M. Á. Herrero, J. D. M. Muñoz, S. Giordani, A. Díaz-Ortiz, S. Filippone, G. Ruaro, M. Meneghetti, M. Prato and E. Vázquez, *J. Am. Chem. Soc.,* 2007, **129**, 14580-14581.

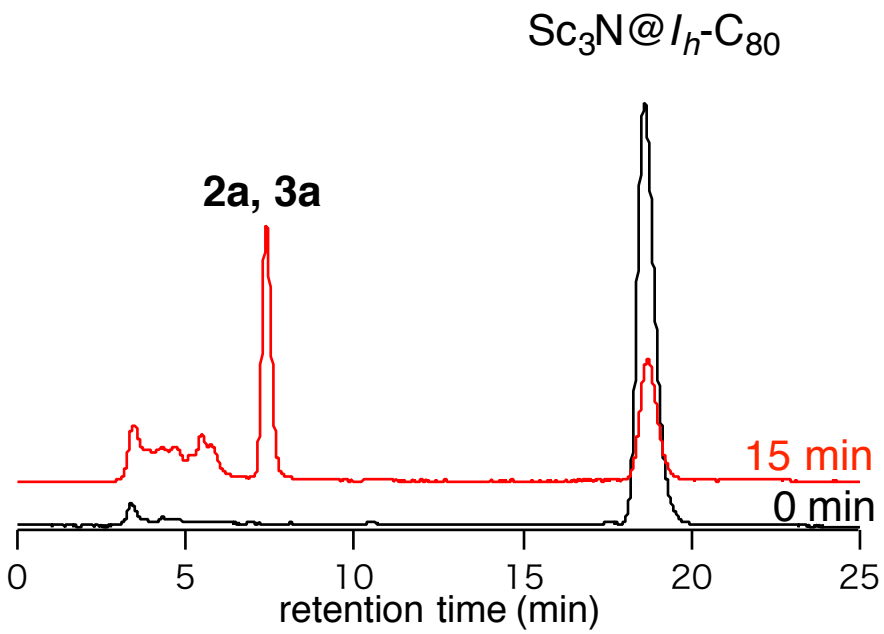

Fig. S1 HPLC profiles of reaction mixture of $Sc_3N@I_h$-C_{80} with **1a** (red). Conditions: 4.6 mm × 250 mm i.d. 5PYE columns; eluent, toluene 1.0 mL/min.

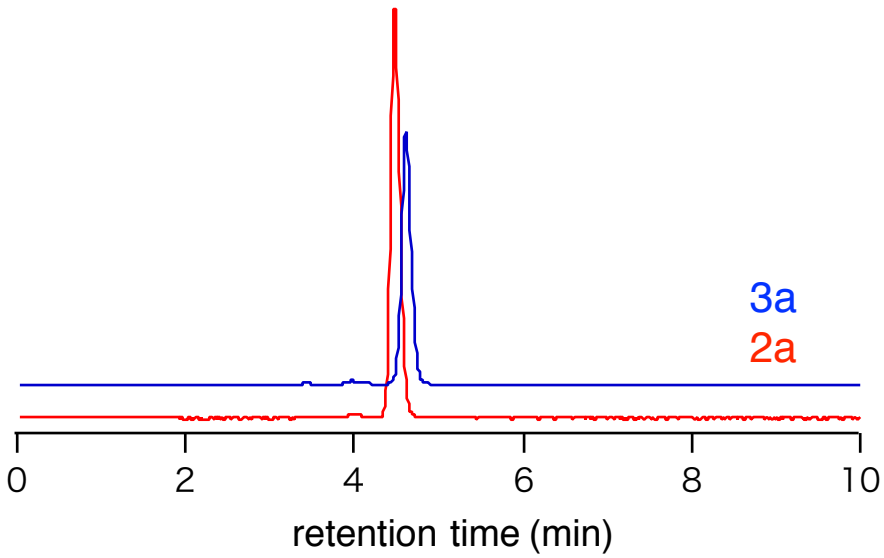

Fig. S2 HPLC profiles of **2a** and **3a**. Conditions: 5NPE column, toluene 1.0 mL min^{-1}, 330 nm detection

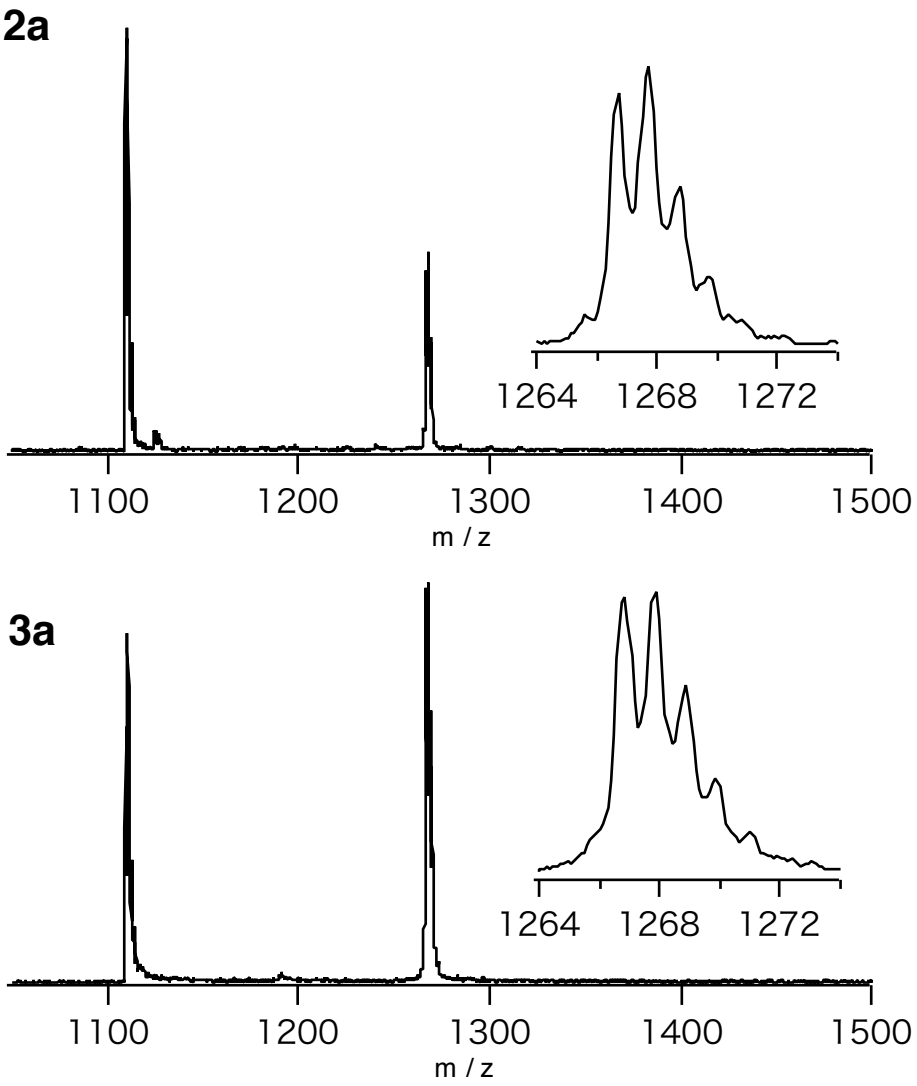

Fig. S3 Mass spectra of **2a** and **3a** in negative mode using TPB as a matrix.

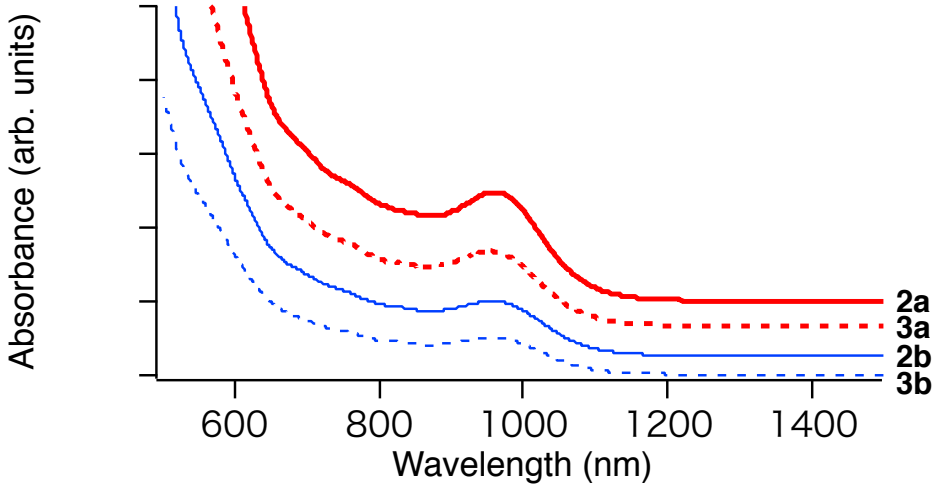

Fig. S4 Absorption spectra of **2** and **3** in CS2.

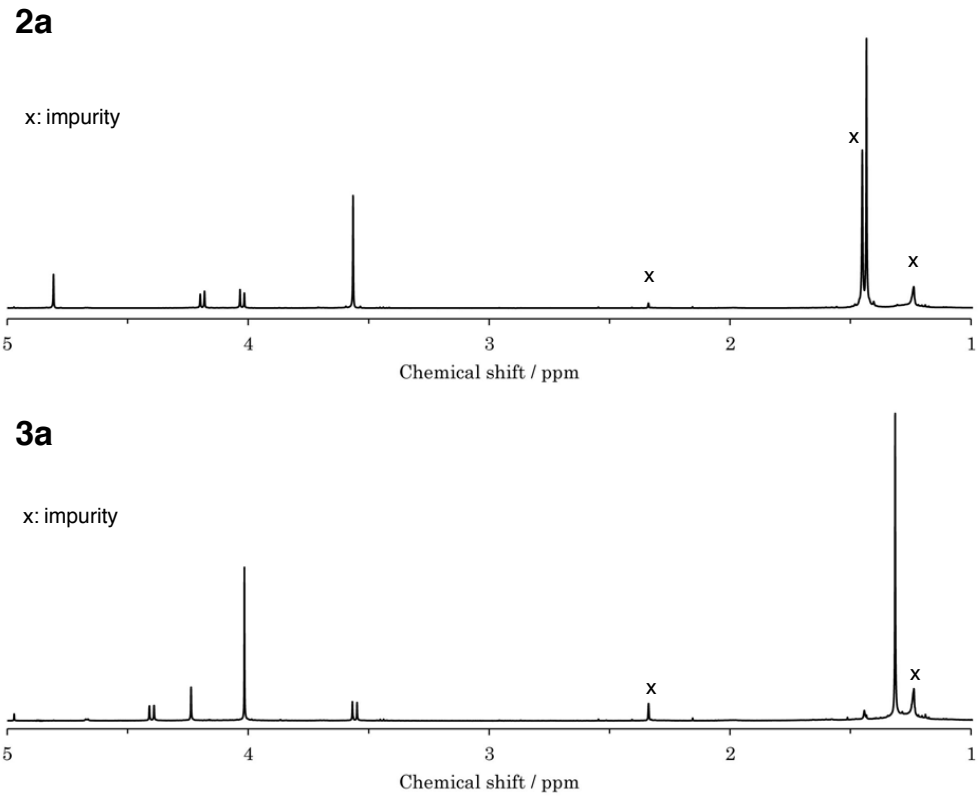

Fig. S5 ^{1}H NMR spectra of **2a** and **3a** in $CDCl_3$:CS_2 = 1:1 (v/v), 125 MHz, 293 K.

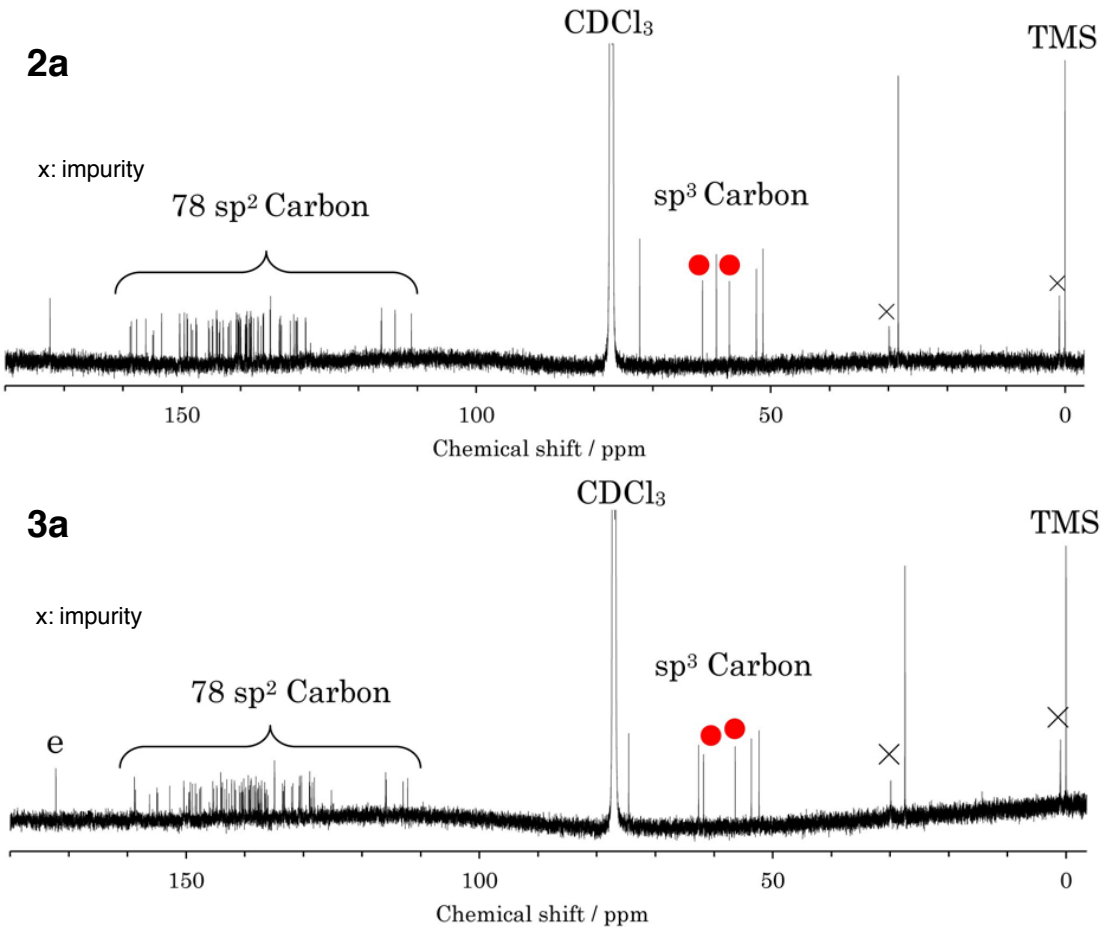

Fig. S6 ^{13}C NMR spectra of **2a** and **3a** in $CDCl_3$:CS_2 = 1:1 (v/v), 125 MHz, 293 K.

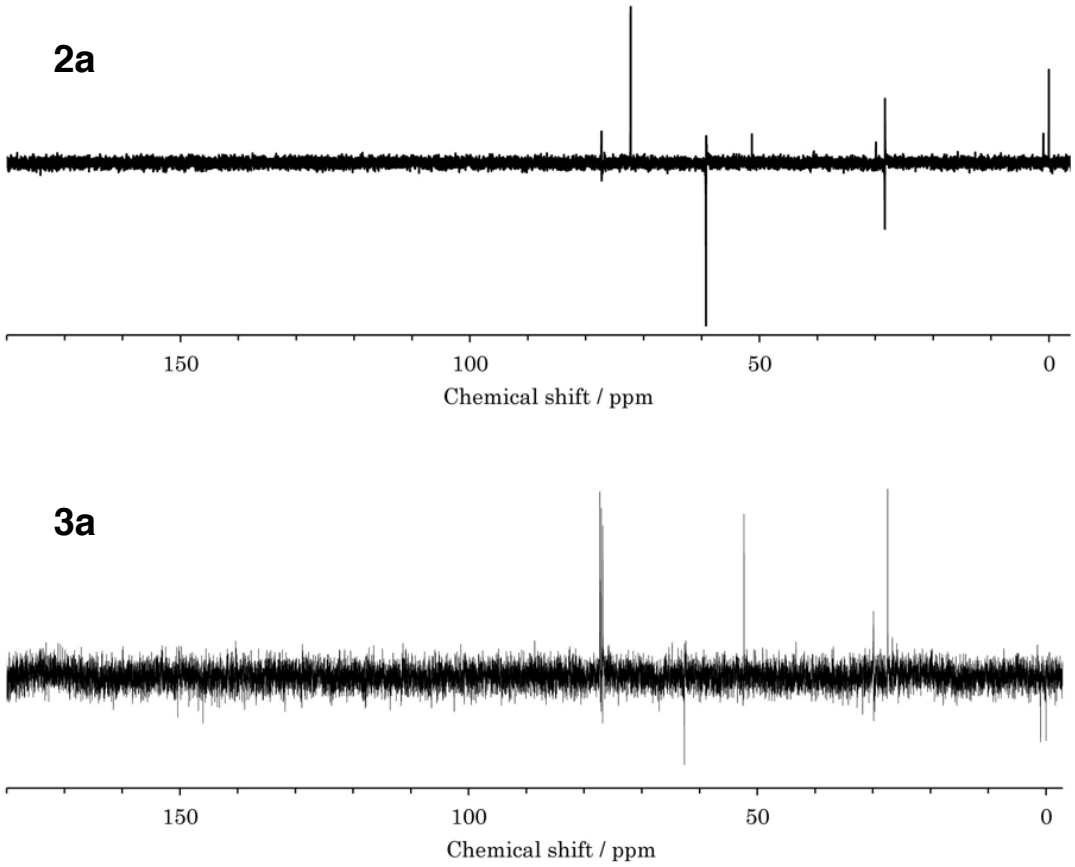

Fig. S7 DEPT-135 NMR spectra of **2a** and **3a** in $CDCl_3$:CS_2 = 1:1 (v/v), 125 MHz, 293 K.

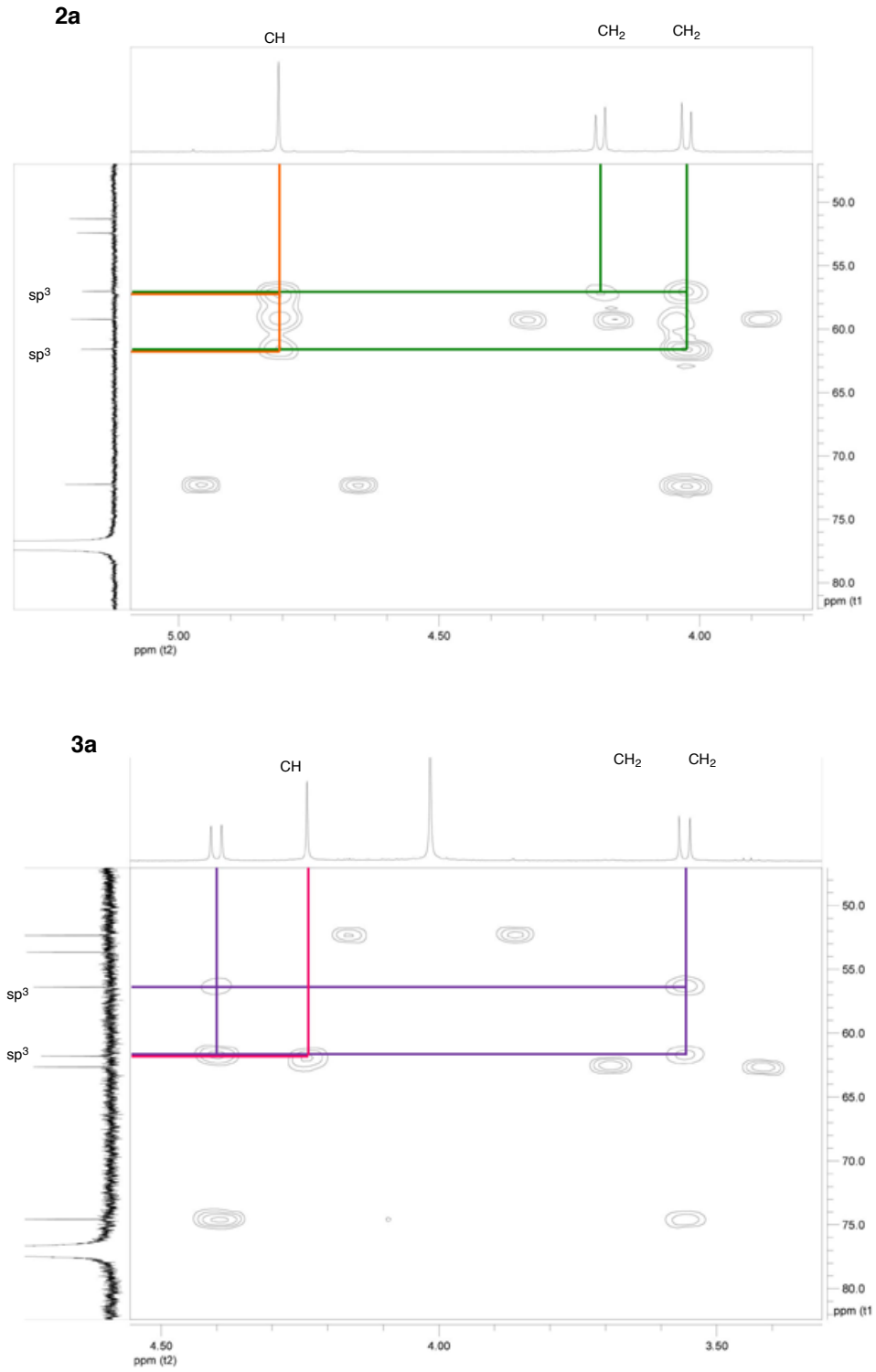

Fig. S8 HMBC spectrum of **2a** and **3a** in $CDCl_3$:CS_2 = 1:1 (v/v), 125 MHz, 293 K.

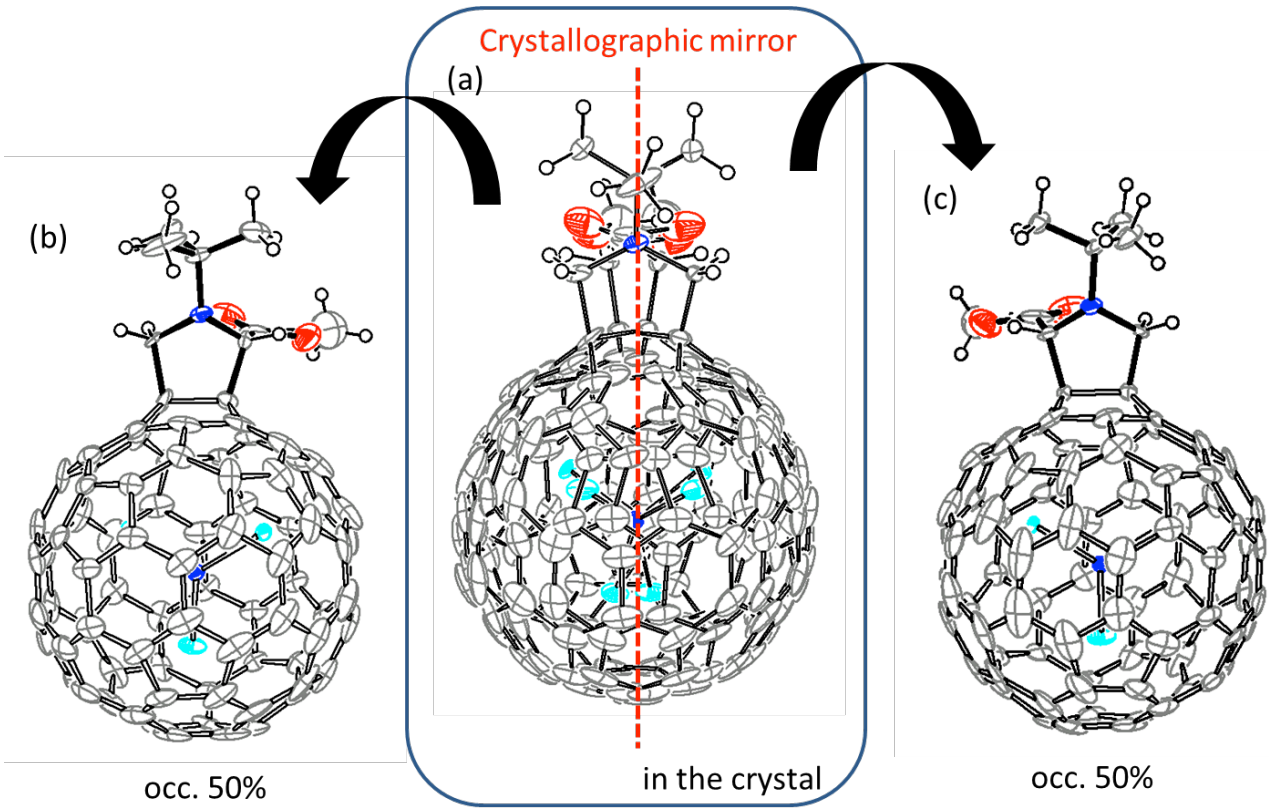

Fig. S9 Drawings of (a) the independent unit (**2a**) in the unit cell that exists on the crystallographic mirror and (b & c) two disorder orientations of the independent unit. Their orientations have the relation of chiral and 0.50 occupancies, respectively.

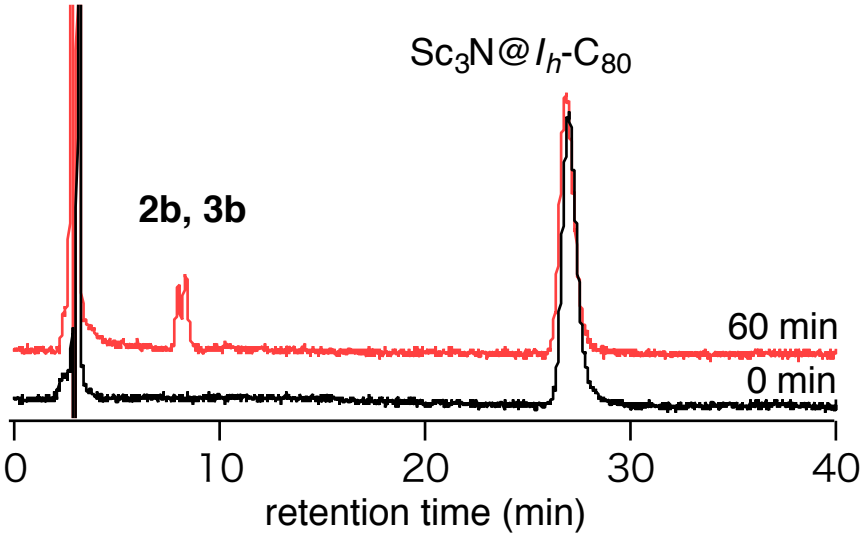

Fig. S10 HPLC profiles of reaction mixture of $Sc_3N@I_h$-C_{80} with **1b** (red). Conditions: 4.6 mm × 250 mm i.d. Buckyprep-M columns; eluent, toluene 1.0 mL/min.

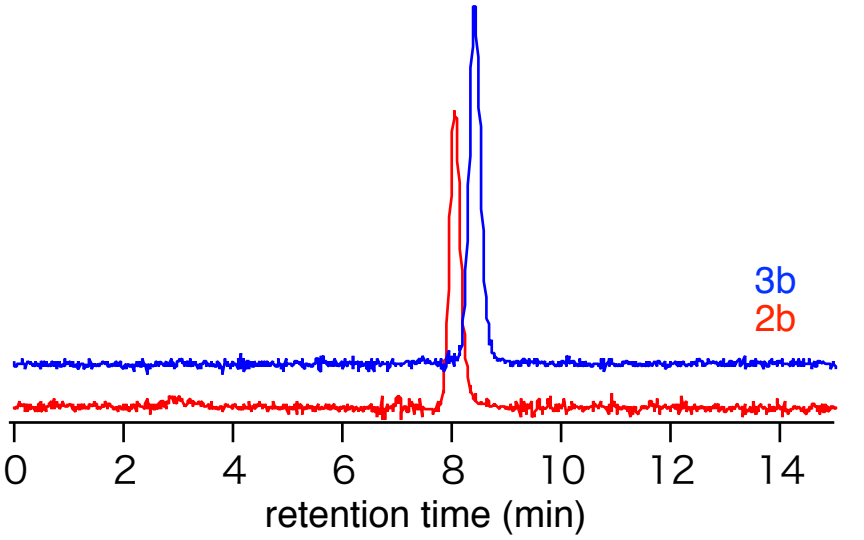

Fig. S11 HPLC profiles of **2b** and **3b**. Conditions: 5NPE column, toluene 1.0 $mLmin^{-1}$, 330 nm detection.

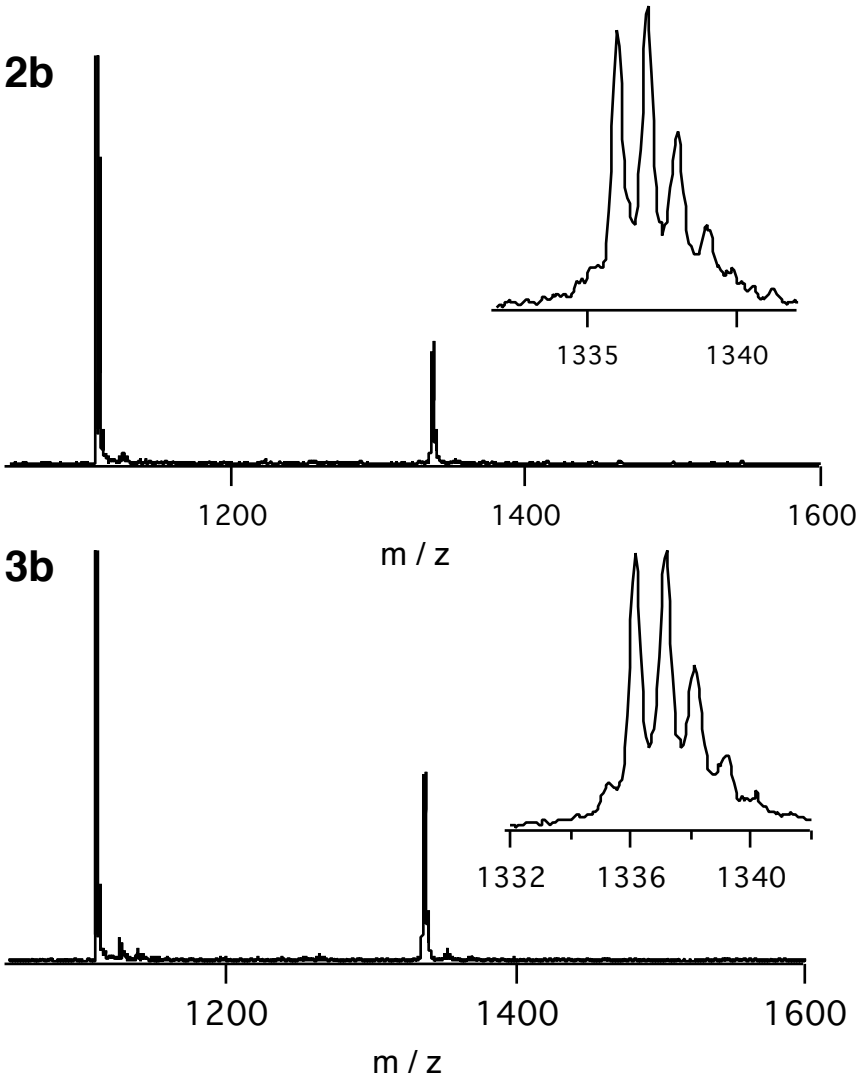

Fig. S12 Mass spectra of **2b** and **3b** in negative mode using TPB as a matrix.

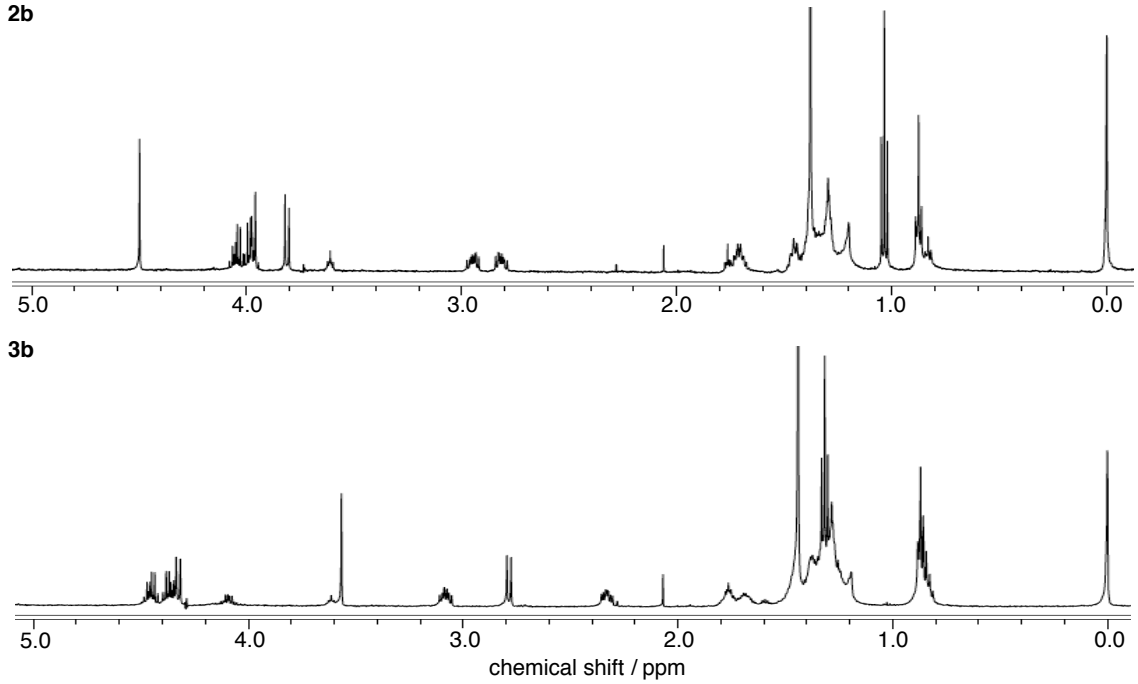

Fig. S13 ^{1}H NMR spectra of **2b** and **3b** in $CDCl_3$:CS_2 = 1:1 (v/v), 400 MHz, 298 K.

2b

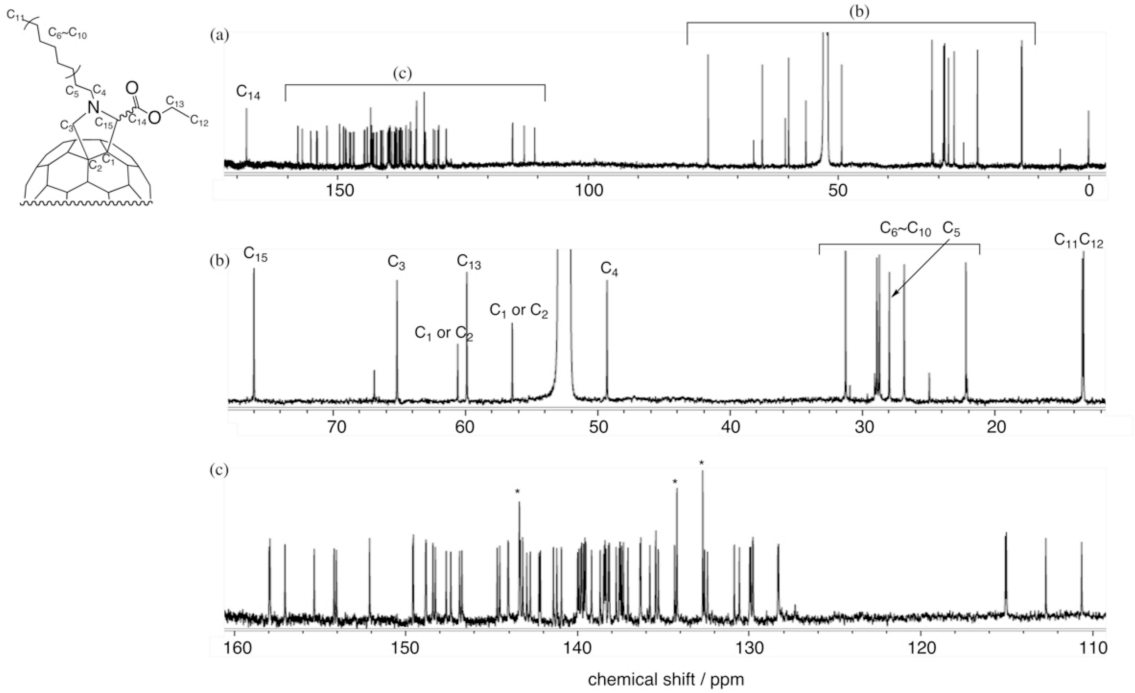

3b

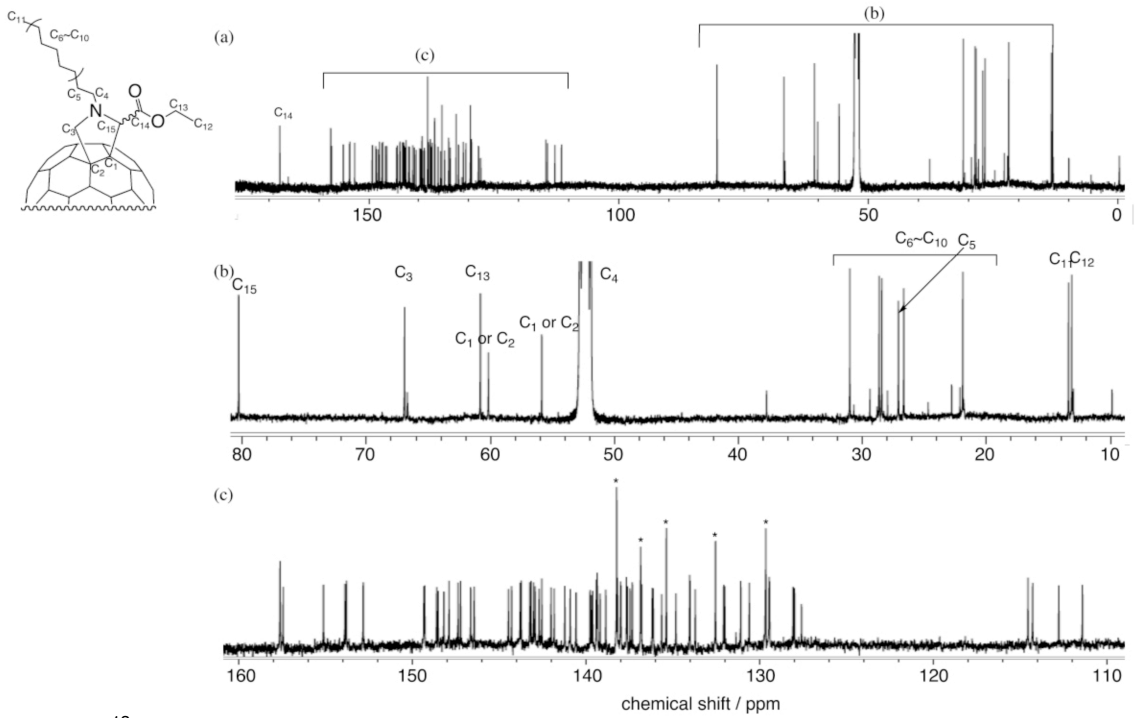

Fig. S14 ^{13}C NMR spectra of **2b** and **3b** in $CDCl_3$:CS_2 = 1:1 (v/v), 125 MHz, 298 K.

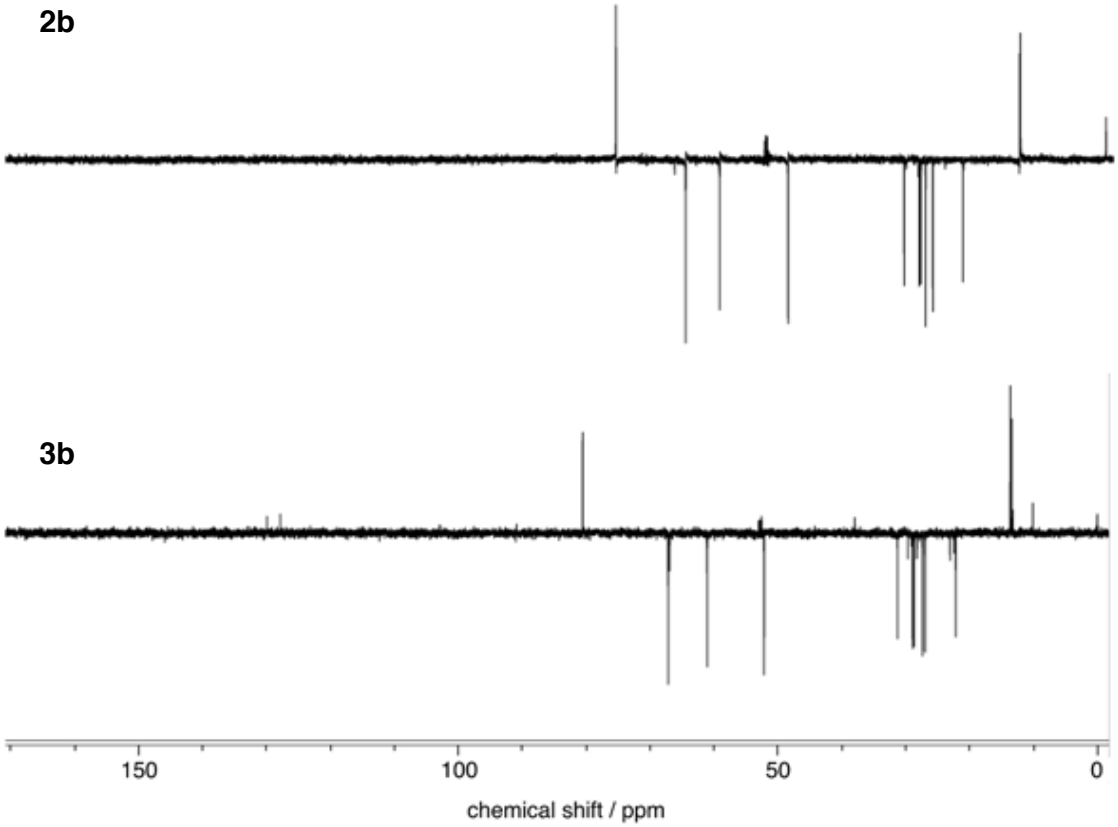

Fig. S15 DEPT-135 ^{13}C NMR spectra (125 MHz) of **2b** and 3**b** measured in $CS_2/CDCl_3$ (1:1) at 298K.

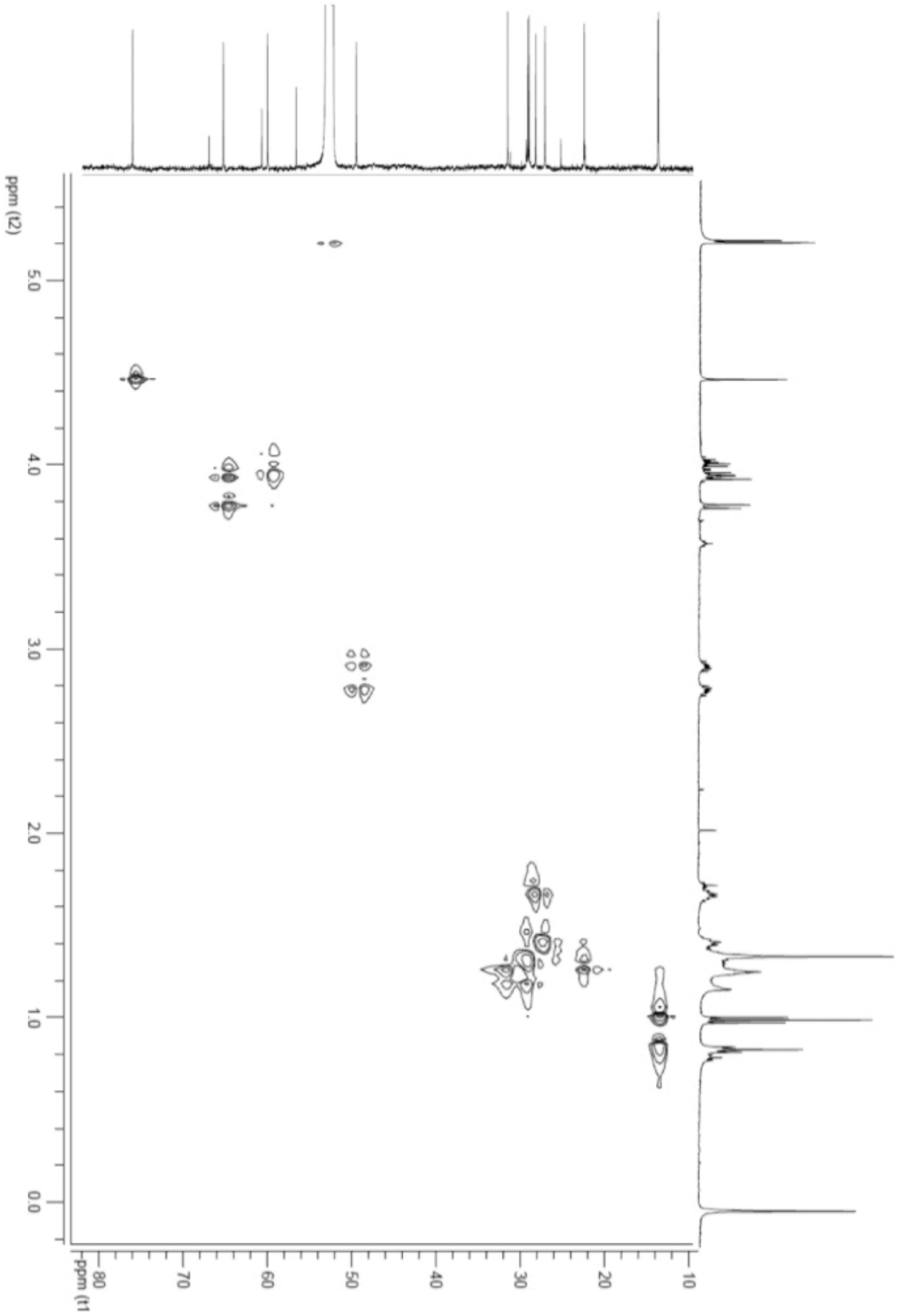

Fig. S16 HSQC NMR spectrum of **2b** measured in $CS_2/CDCl_3$ (1:1) at 298K.

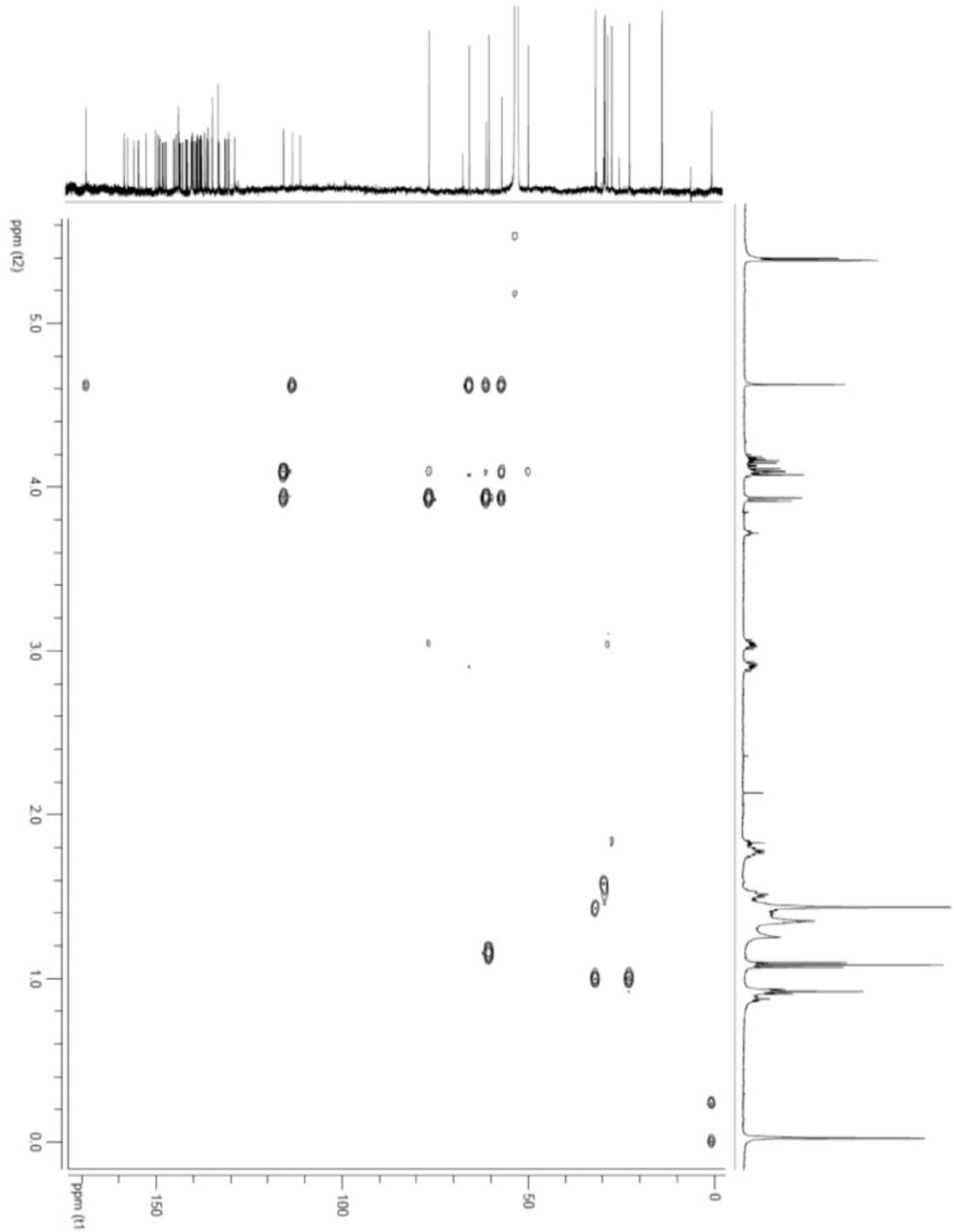

Fig. S17 HMBC NMR spectrum of **2b** measured in $CS_2/CDCl_3$ (1:1) at 298K.

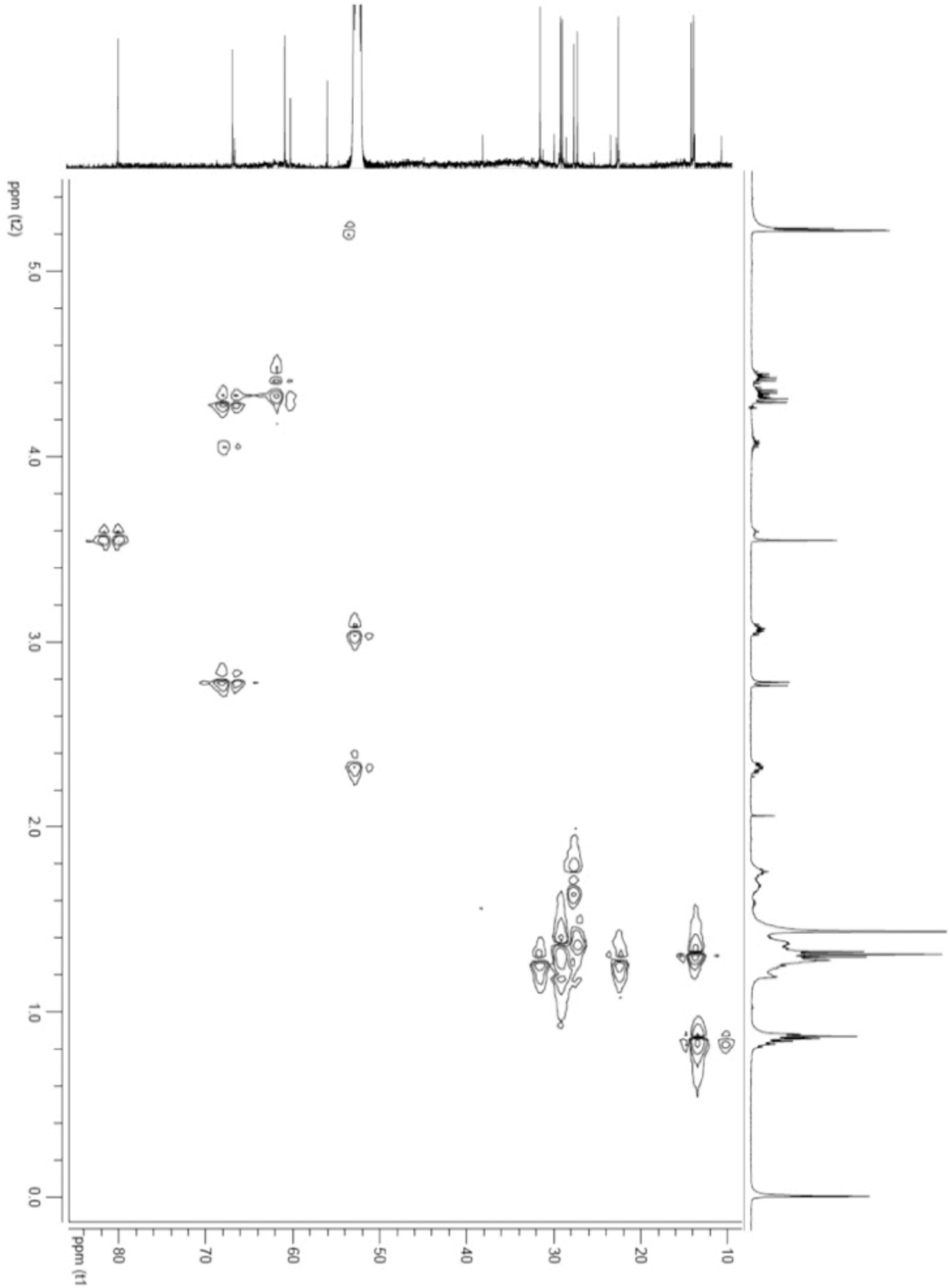

Fig. S18 HSQC NMR spectrum of **3b** measured in $CS_2/CDCl_3$ (1:1) at 298K.

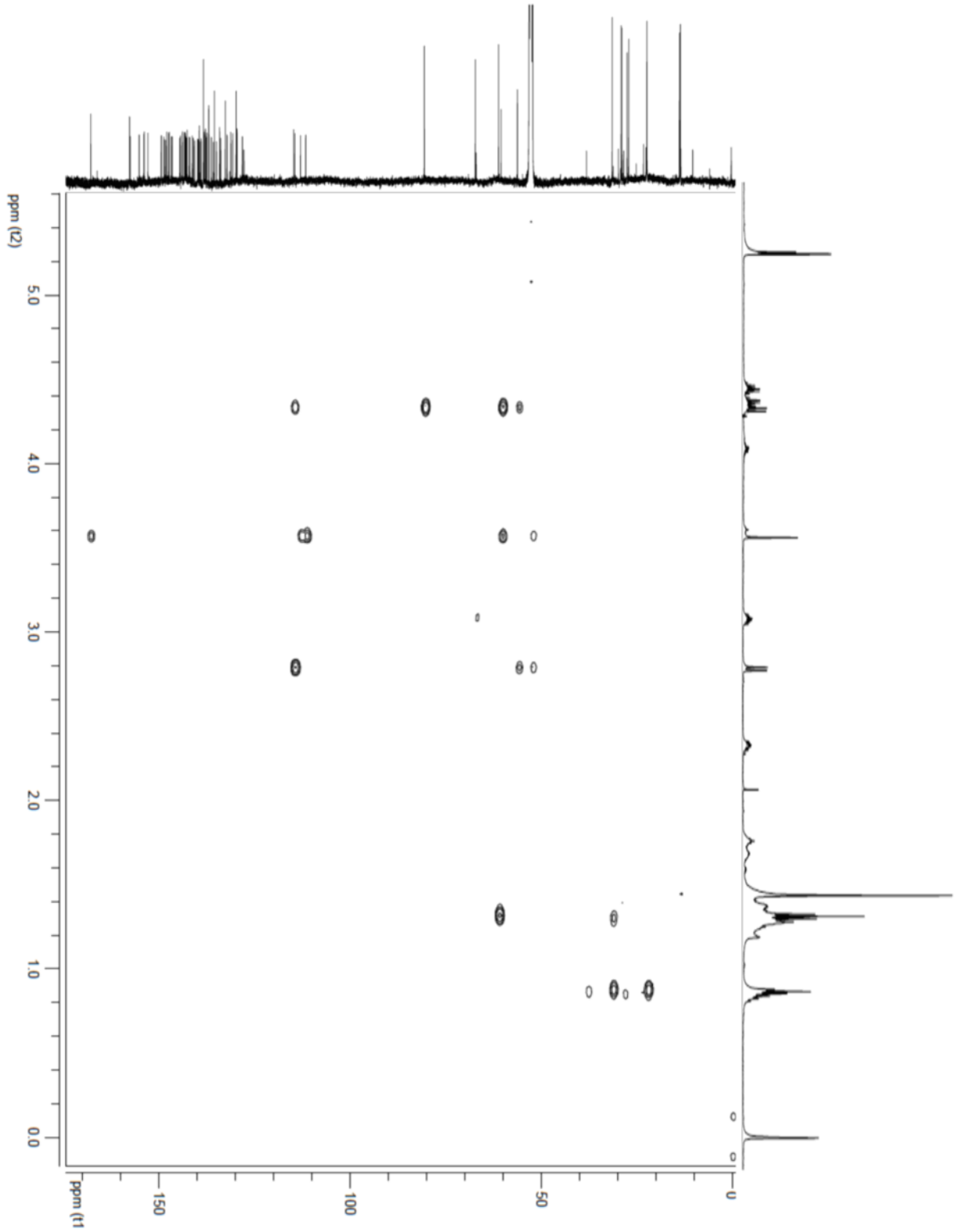

Fig. S19 HMBC NMR spectrum of **3b** measured in $CS_2/CDCl_3$ (1:1) at 298K.

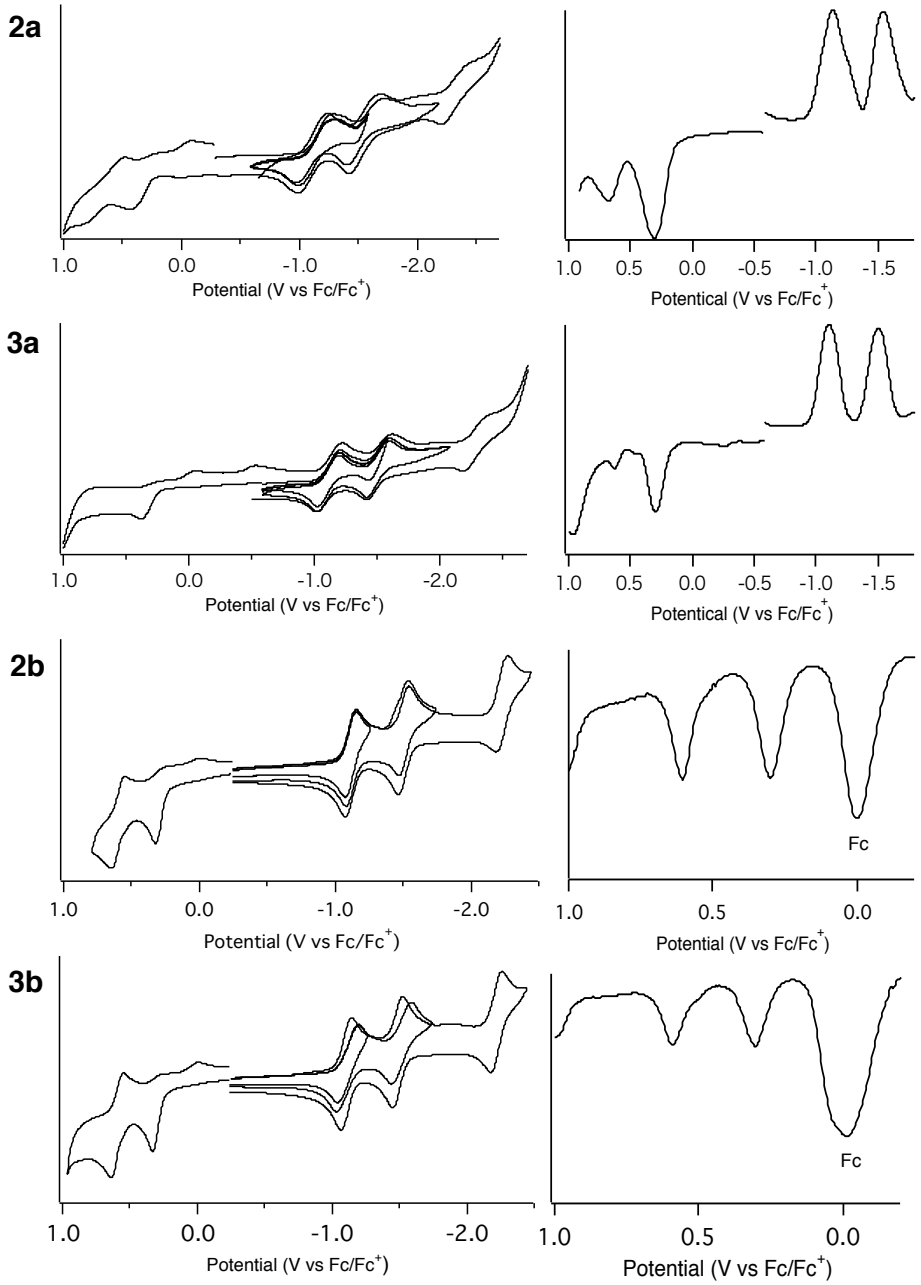

Fig. S20 CV and DPV curves of **2a**, **2b**, **3a**, and **3b** in ODCB.

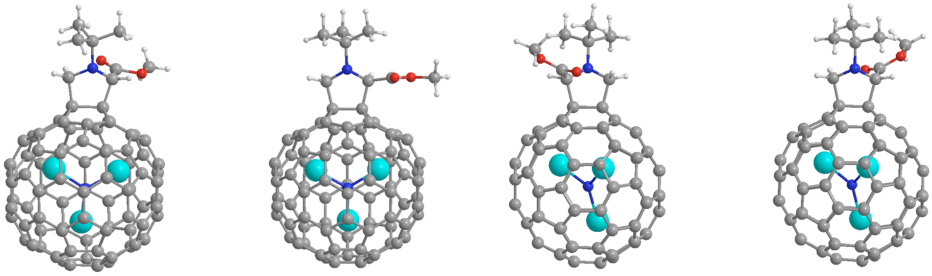

Addition type	A (**2a**)	B (**3a**)	C	D
Relative energy	0 kcal/mol	+2.16 kcal/mol	+9.45 kcal/mol	+9.36 kcal/mol

Fig. S21 Optimized structures for [5,6]- and [6,6]-pyrrolidino-$Sc_3N@I_h$-C_{80} calculated at M06-2X/6-31G(d)[C,H,N,O], LanL2DZ[Sc] level.

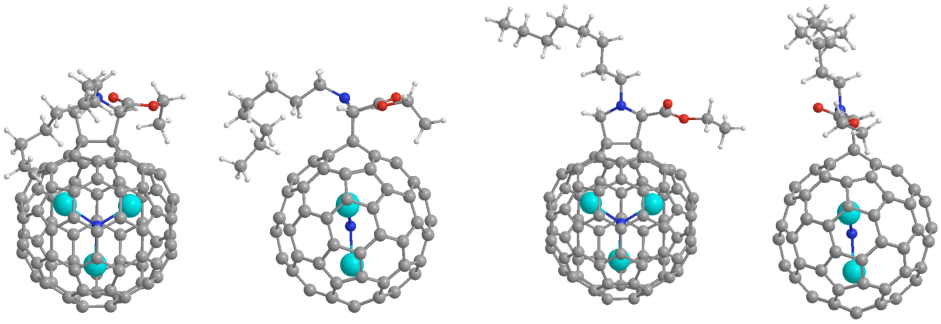

	front view	side view	front view	side view

Addition type	A (**2b**)	B (**3b**)
Relative energy	0.53 kcal/mol	+0.00 kcal/mol

Fig. S22 Optimized structures for [5,6]- and [6,6]-pyrrolidino-$Sc_3N@I_h$-C_{80} calculated at M06-2X/6-31G(d)[C,H,N,O], LanL2DZ[Sc] level.

Retro-cycloaddition reaction of multi-addition products.

We conducted retro-cycloaddition reaction of (pyrrolidino)$_n$-$Sc_3N@I_h$-C_{80}, which was generated as a by-product, for recycling of the metallofullerene. (pyrrolidino)$_n$-$Sc_3N@I_h$-C_{80} was prepared from $Sc_3N@I_h$-C_{80} and **1b**. (pyrrolidino)$_n$-$Sc_3N@I_h$-C_{80} was heated with maleic anhydride at 180˚C for 24 h to give $Sc_3N@I_h$-C_{80} in a yield of 53 %, which was estimated by using HPLC analysis, based on the consumption of $Sc_3N@I_h$-C_{80} in 1,3-dipole cycloaddition reaction.

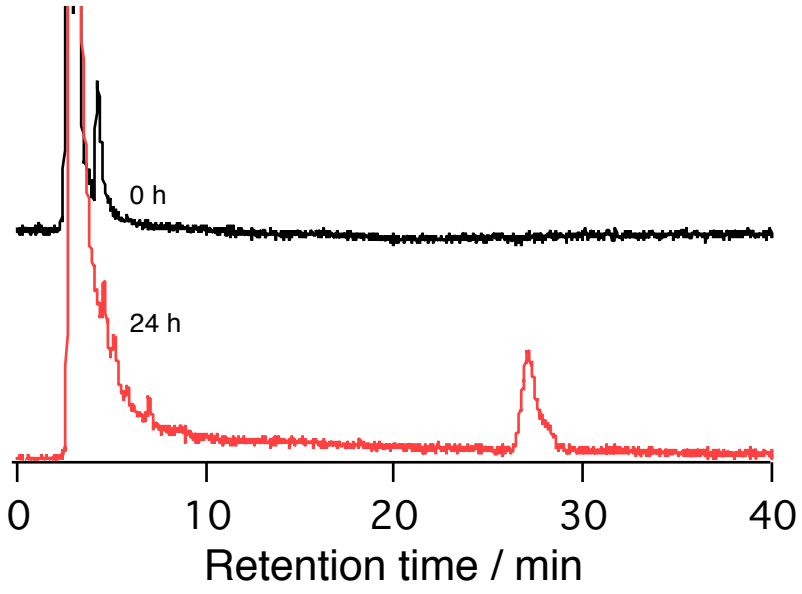

Fig. S23 HPLC profiles of (pyrrolidino)$_n$-$Sc_3N@I_h$-C_{80} in the presence of maleic unhydride at 180˚C for 24 h. Column: Buckyprep 4.6 ϕ × 250 mm, 40°C, eluent: toluene 1.0mL/min.

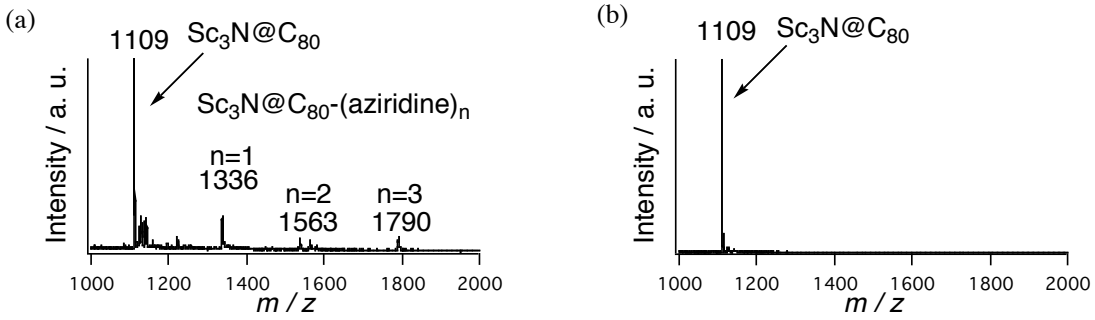

Fig. S24 Negative-mode MALDI-TOF mass spectra of (a) (pyrrolidino)$_n$-$Sc_3N@I_h$-C_{80} and (b) (pyrrolidino)$_n$-$Sc_3N@I_h$-C_{80} treated at 180˚C for 24 h in the presence of maleic unhydride. matrix: 1,1,4,4-tetraphenyl-1,3-butadiene.